Advances in Concrete Construction, *Vol. 16, No. 0 (2023) 000-000*
https://doi.org/10.12989/acc.2023.16.0.000

Effect of parameters on the tensile behaviour of textile-reinforced concrete composite: A numerical approach

Tien M. Tran*[1], Hong X. Vu [2a] and Emmanuel Ferrier [2b]

[1] *Department of Mechanisms of Materials, Hanoi University of Mining and Geology (HUMG), n°18 Vien street, Duc Thang ward, Bac Tu Liem district, Ha Noi city, Vietnam*
[2] *Laboratoire des Matériaux Composites pour la Construction LMC2, Université de LYON, Université Claude Bernard LYON 1, France*

(*Received August 8, 2022, Revised September 29, 2023, Accepted October 31, 2023*)

Abstract. Textile-reinforced concrete composite (TRC) is a new alternative material that can satisfy sustainable development needs in the civil engineering field. Its mechanical behaviour and properties have been identified from the experimental works. However, it is necessary for a numerical approach to consider the effect of the parameters on TRC's behaviour with lower analysis duration and cost related to the experiment. This paper presents obtained results of the numerical modelling for TRC composite using the cracking model for the cementitious matrix in TRC. As a result, the TRC composite exhibited a strain–hardening behaviour with the cracking phase characterized by the drops in tensile stress on the stress-strain curve. This model also showed the failure mode by multi-cracking on the TRC specimen surface. Furthermore, the parametric studies showed the effect of several parameters on the TRC tensile behaviour, as the reinforcement ratio, the length and position of the deformation measurement zone, and elevated temperatures. These numerical results were compared with the experiment and showed a remarkable agreement for all cases of this study.

Keywords: cracking model; numerical modelling; parametric study stress-strain curve; textile-reinforced concrete

1. Introduction

Fiber reinforced polymer (FRP) and textile-reinforced concrete (TRC) composites are new alternative materials that can satisfy sustainable development needs in the civil engineering field. With their remarkable mechanical properties, these materials have been used to reinforce and/or strengthen the element structures (RC members, masonries, slabs, columns, …) (Brameshuber 2006, Mechtcherine 2013, Halim *et al*. 2021). However, TRC composite is considered as the construction material for the future thanks to sustainability and environmental friendliness. So, for a better understanding of this material, the experimental works were performed in the literature to characterize its tensile behaviour and mechanical properties. According to the results in the previous experimental works, this material exhibited a strain-hardening behaviour with three phases depending on several different factors (Giese *et al*. 2021, Caggegi *et al*. 2017, Li *et al*. 2019). It also has been tested to identify its performance for an application in some cases of the special environment as elevated temperature or ageing conditions (Portal *et al*. 2016, Tran *et al*. 2019). In order to identify the mechanical properties of the TRC composite, the notation points in the idealized stress-strain curve were defined (Tran *et al*. 2019, 2021). Three points, corresponding respectively to the beginning of the cracking (point I), the end of the cracking (point II), and the rupture of the specimen (UTS – Ultimate Tensile Strength point), are divided into three phases of strain-hardening behaviour of TRC composite. The stress and strain corresponding with these points and the tangent of the idealized stress-strain curve in each phase identified the mechanical properties of the TRC composite (Tran *et al*. 2019, 2021). However, in order to consider the effect of the factors belonging from the reinforcement textile and the cementitious matrix to these properties, it needs more experimental studies.

Over the past recent decades, the numerical approach was used to solve complex problems that could not be performed in the experiment or could be with high cost and time. The finite element method was the most powerful and reasonable choice for several case study. For example, 3D finite element modeling in Atena-Gid 3D software could predict the shear behaviour of steel fibre reinforced concrete haunched beams and take into account the effect of steel fiber volumetric ratio on this behaviour (Jawahery *et al*. 2022). For the case study in this paper, a 3D finite element model could estimate the global and local behaviour of the TRC composite as well as its constitutive materials (Tran *et al*. 2020a, b). The following paragraphs present the previous research, which focuses on the numerical behaviour of the TRC composite and the effect of the studied parameters on its behaviour. The objective of this study is presented at the end of the introduction of this paper.

*Corresponding author, Ph.D.,
E-mail: tranmanhtien@humg.edu.vn
[a] Associate Professor, E-mail: xuan-hong.vu@univ-lyon1.fr
[b] Professor, E-mail: emmanuel.ferrier@univ-lyon1.fr

ISSN: 2287-5301 (Print), 2287-531X (Online)

1.1 Numerical studies on the mechanical behaviour of TRC and TRC strengthened structures

In the literature, several numerical models were developed and validated to consider many factors belonging to constitutive materials (Tran *et al*. 2020b, Portal *et al*. 2017, Djamai *et al*. 2017, Rambo *et al*. 2017, Colombo *et al*. 2018, Li *et al*. 2020). Portal *et al*. (2017) have modified the width/thickness ratio of textile yarns to find the effect of the contact perimeter between carbon textile yarns and cementitious matrix. Djamai *et al*. (2017) have considered all the possible failure mechanisms of the constitutive materials (cracking of cementitious matrix and debonding between textile/matrix) in multi-scale numerical modelling for the TRC sandwich panel from the pull-out response of textile yarn in the cementitious matrix block to the four points bending behaviour of TRC sandwich panel. The effect of the bond-slip response on the shape of stress-strain curves and crack spacing in the residual tension stiffening behaviour of TRC specimens after exposure to the elevated temperature of pre-heating has been studied by Rambo *et al*. (2017). Li *et al*. (2020) have investigated the influences of different factors (the axial compression ratio, shear span ratio, and concrete strength grade) on the seismic performance of textile-reinforced concrete (TRC)-strengthened reinforced concrete (RC) columns. The effect of material parameters on the mechanical properties of TRC sandwich beams in four-point bending has been analyzed and discussed in the analytical and numerical study of Colombo *et al*. (2018). Douk *et al*. (2021) have studied the effects of TRC thickness and thermal loading rate on the thermomechanical behaviour of RC beams with and without TRC strengthening. All these numerical results were in good agreement with that in the experiment and significantly contributed to our knowledge for numerical modelling on the mechanical behaviour of TRC and TRC strengthened- structures.

Concerning the numerical model for TRC material, it needs to use the cracking model for the cementitious matrix. This model has been successfully used in several previous studies to show the failure mode with multi-cracks on the surface (Tran *et al*. 2021, Djamai *et al*. 2017). In the literature, two main approaches were used for the simulation of the non-linear behaviour of the cementitious matrix considering its crushing and cracking (Tran *et al*. 2021, William and Warnke 1975). The first is a discrete cracking approach, which considers the crack as a discontinuity of the material at the position of the cracking planes. The second is a homogenized approach which gives a global behaviour of the matrix in tension without taking into account the explicit opening of cracks (William and Warnke 1975). Therefore, it is commonly used today because it allows keeping the original mesh and does not impose a priori constraints on the orientation of the cracks (Tran *et al*. 2021, Truong 2016).

1.2 Effect of studied parameters on the TRC's behaviour

To characterize the TRC's behaviour and mechanical properties, an important factor that influences significantly the experimental result was the method of strain measurement. The LVDTs (Linear Variable Differential Transformer) were the most useful for this material and generally provided a reliable strain result (Colombo *et al*. 2013, Contamine *et al*. 2011). However, in some cases of difficulty as too small specimens or at an elevated temperature, this contact measurement method could not be used. Therefore, several high-technical measurement methods as DIC (Digital Image Correlation), laser sensor, or optical fiber have been efficiently used for these difficult cases (Caggegi *et al*. 2017, Tlaiji *et al*. 2018, Tran *et al*. 2019, Saidi and Gabor 2019). However, even if these high-technical measurement instruments have been set up for experimental work, the strain result still was influenced by the position and length of the strain measurement zone. Furthermore, the complex cracking response of the cementitious matrix could significantly affect the local and global behaviour of the TRC specimens. The experimental result of Saidi and Gabor (2020) showed the difference in the strain-stress relationship curves of the cementitious matrix in both observed regions: cracked and uncracked ones. So, it is necessary to identify the effect of the length and position of the strain measurement zone on the shape and the number of cracks of the stress-strain curve.

Another important factor that influences the mechanical behaviour of the TRC composite is the reinforcement ratio. In the literature, there were several experimental studies on TRC material concerning the effect of this parameter (Caggegi *et al*. 2017, Colombo *et al*. 2013, Ferrara *et al*. 2019). This effect could be explained by the effectiveness of one reinforcement layer for the thickness of the cementitious matrix layer, essentialy depending on two main factors. Firstly, it depends on the together working between the textile layers, leading it possible to the weakness of the textile-matrix bond. Secondly, the cementitious matrix thickness surrounding a textile layer can make it possible to correctly transfer the internal force between the textile layers (Truong 2016). In the work of Rambo *et al*. (2014), the different reinforcement ratios (by 1, 3, and 5 layers of basalt textile) of the basalt TRC presented different shapes of mechanical behaviour as well as the ultimate strength. As result, the ultimate tensile strength improved respectively 1.01, 1.2, and 2.6 times compared to that of the un-reinforced cementitious matrix. Hence, the effectiveness of one reinforcement layer for the thickness of the cementitious matrix layer needs also to be studied for a better understanding of TRC material.

In the last decade, the TRC composite has been tested to replace the fiber-reinforced polymer (FRP) composite for strengthening the RC members in the case of fire. So, the effect of the elevated temperature on the TRC's behaviour and its mechanical properties was identified by the thermomechanical tests in several studies (Tlaiji *et al*. 2018, Rambo *et al*. 2014, Ehlig *et al*. 2010) studies (Tlaiji *et al*. 2018, Rambo *et al*. 2014, Ehlig *et al*. 2010). As result, the mechanical performance of TRC gradually decreased and depended totally on the capacity of reinforcement textile at the temperature level lower than 400°C. For a thermomechanical test setup, it needs a lot of instruments as

the furnace for the temperature heating, the thermocouples for the temperature control, and a high-technical measurement method for strain measurement. So, a sole experimental approach could not be adopted because it costs time and finance. With the experimental required data, a numerical approach is a reasonable choice to study the effect of the elevated temperature on the thermomechanical behaviour of the TRC composite (Tran *et al*. 2020).

1.3 Objective of this study

To the best of the authors' knowledge, rare existing results consider the effects of several factors, concerning the strain measurement zone, the effective thickness of the cementitious matrix for a textile layer, and the elevated temperature, on the global behaviour of TRC composite. So, this study aims to contribute additionally to the knowledge concerning the effect of these studied parameters by using a numerical approach. In this paper, the 3-D numerical model was built in Ansys ADPL for TRC composite by using the cracking model for the cementitious matrix. Firstly, this model was developed and validated with the previous experimental data on the tensile behaviour of carbon TRC composites. This model was then used to study the effect of several parameters mentioned above. The effect of the position and length of the strain measurement zone would be highlighted thanks to the record of the displacement of all nodes in the 3-D model. The effect of the effective cementitious matrix thickness for a textile layer would be identified by changing its value in the model. Finally, the evolution of the TRC's mechanical behaviour and its properties with the elevated temperature would be determined. All numerical results would be analyzed and discussed in this paper.

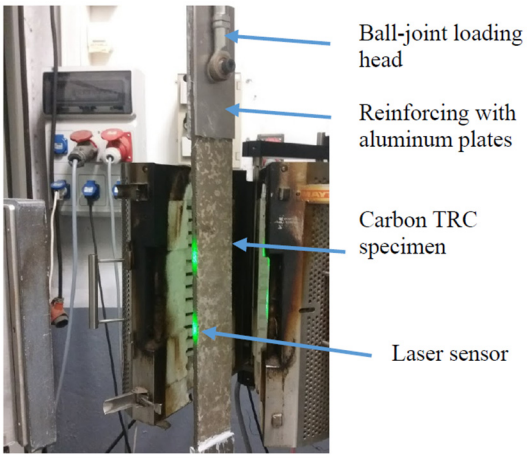

Fig. 1 Experimental works for the validation of 3-D model (Tran *et al*. 2020, Tran 2019)

2. Numerical approach

This section presents the numerical works including the development and validation of 3-D numerical model.

2.1 Experimental data

The experimental results in the literature were used for the development and validation of the 3-D numerical model. These were the tensile behaviour and mechanical properties of two carbon TRC composites (F.GC1 and F.GC2) at room temperature in the thesis of Tran (2019). Concerning this experiment, Fig. 1 shows the characterization method of the experimental works for the tensile behaviour of both carbon TRCs. The mechanical properties of constitutive materials (carbon textiles and cementitious matrix) were also identified from this method. The input data of the numerical model so was chosen from these results. Table 1 presents all the input data for the numerical model.

2.2 Numerical model properties

2.2.1 Dimension of the 3-D model

The numerical model was constructed step by step in Ansys APDL with the dimension of a half sample (as in the experimental work) thanks to the symmetry of loading, boundary conditions, and materials. Firstly, a block of the cementitious matrix with a dimension depending on the type of carbon TRC (see Fig. 2(a)) was created and declared as the SOLID65 element in the model. Then, the longitudinal textile yarns were also added in their position as in the real TRC specimen with the definition as reinforcement rebar (Link180 element). For the validation of the 3-D model, two types of carbon TRC composite with a different configuration of carbon textile were used: GC1 carbon textile for F.GC1 composite and GC2 carbon textile for F.GC2 composite. Fig. 2 presents the dimension of carbon TRC specimens in the experiment and corresponded models with the use of the elements for carbon textile and the cementitious matrix.

Table 1 Mechanical properties of carbon textiles and cementitious matrix for numerical model (Tran 2019)

TRC composite	Reinforcement textile			Cementitious matrix		
	Describe of materials	Young's modulus (GPa)	Tensile strength (MPa)	Describe of materials	Young's modulus (GPa)	Tensile strength (MPa)
F.GC1	Carbon textile GC1	256	2617	Fine-grained cementitious matrix	8.41	5.29
F.GC2	Carbon textile GC2	144	1312	Fine-grained cementitious matrix	8.41	5.29

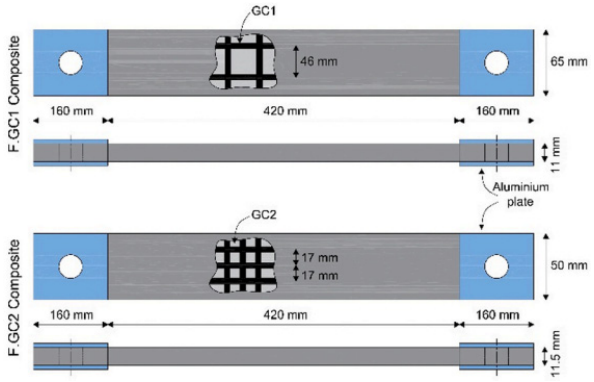

(a) In experimental works

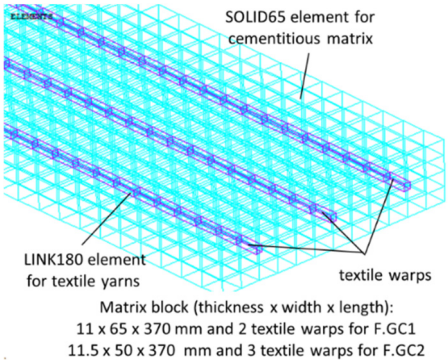

(b) In 3-D model

Fig. 2 Dimension of carbon TRC specimens in the experimental works and 3-D model

2.2.2 Cracking model for cementitious matrix

The material model for the cementitious matrix was used in this numerical study, called CONCR - Nonlinear Behaviour – Concrete. This model could take into account the cracking behaviour by a criterion of failure due to a multiaxial stress state (William and Warnke 1975). The criterion for the failure of concrete due to a multiaxial stress state can be expressed in the following equation

$$\frac{F}{f_c} - S \geq 0 \qquad (1)$$

where F is a function of the principal stress state ($\sigma_{xp}, \sigma_{yp}, \sigma_{zp}$), depending on the failure surface; S is failure surface expressed in terms of principal stresses and five input parameters f_t (ultimate uniaxial tensile strength), f_c (ultimate uniaxial compressive strength), f_{cb} (ultimate biaxial compressive strength), f_1 (ultimate compressive strength for a state of biaxial compression superimposed on hydrostatic stress state) and f_2 (ultimate compressive strength for a state of uniaxial compression superimposed on hydrostatic stress state), f_c is uniaxial crushing strength. If the mentioned equation above is satisfied, the material will crack or crush.

Fig. 3 below shows the stress-strain relationship of cracking model in the case of cracking in one direction only as the cementitious matrix in TRC composite.

Where: f_t = uniaxial tensile cracking stress; T_c = multiplier for tensile stress relaxation; σ_{ck} = uniaxial tensile cracking strain; R_t = slope (secant modulus) as defined in Fig. 3.

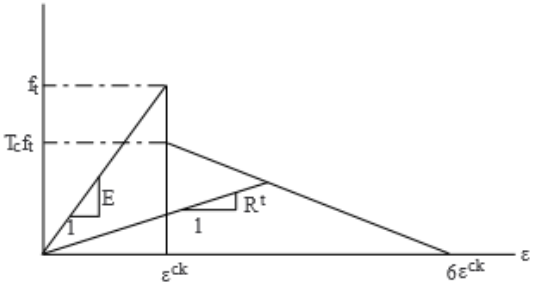

Fig. 3 Stress-strain relationship of the cracking model in the case of cracking in one direction only (ANSYS 2011)

2.2.3 Boundary conditions and loads

The boundary conditions and loads were applied for 3-D model as in the experimental works. In the experiment, two ends of the TRC specimens were reinforced with the aluminium plates to transfer the tensile force and avoid the stress concentration at these positions. So, all the nodes in the talon part of the first end were fixed supports with all movements blocked according to three coordinated axes. Then, all nodes the other end was applied the imposed displacement with the rate of the applied load as in the experiment, controlling by the load steps and sub-steps. Fig. 4 shows the configuration of the boundary condition and applied loading for the numerical model.

2.3 Numerical results

The numerical model could predict the mechanical behaviour of TRC composites, including the stress-strain curve, the mechanical properties, failure modes, and behaviour of constitutive materials.

2.3.1 Strain-hardening curves

Fig. 5 shows the strain-hardening curves of tensile

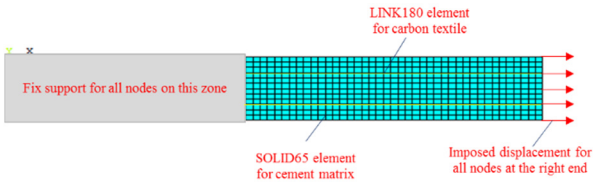

(a) For carbon TRC composite with two textile yarns as reinforcement (F.GC1)

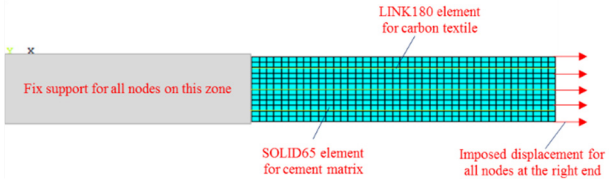

(b) For carbon TRC composite with three textile yarns as reinforcement (F.GC2)

Fig. 4 Numerical models for the carbon TRC specimens

(a) For F.GC1 composite (b) For F.GC2 composite

Fig. 5 Comparison between both experimental and numerical results for strain-hardening curves (Tran 2019)

behaviour for both carbon TRCs with the cracking phase as described in the literature. In Fig. 5, the cracking phase is characterized by the drops in axial stress in the strain-hardening curves. It means that the cracking model for the cementitious matrix simulated the response of this material as in reality. However, for the case of the F.GC1 composite, the first drop in stress was extremely deeper than the next ones. This result was in agreement with the observation of strain-hardening curves in the experiment for this TRC. It was caused by the configuration of carbon textile GC1 in the F.GC1 specimen, there were only two warps of GC1 textile with the distance between themselves of 46 mm. For the case of the F.GC2 composite, a perfect cracking phase was obtained from the 3-D numerical model. It could be explained this result by the reasonable reinforcement of three GC2 textile warps with the distance between themselves of 17 mm. In comparison with experimental results, it could be found a little difference in the second half of the behaviour curve between both experimental and numerical results. This result was caused by the difference in axial deformation due to several phenomena occurring after each crack appearance which will be further analyzed in section 2.4.

2.3.2 Mechanical properties of carbon TRC composites

From the strain-hardening curves in Fig. 5, the mechanical properties of both TRC composites could be identified. Concerning the properties in the first phase, for the F.GC1 specimen, the cracking stress (σ_I) and the initial stiffness (E_I) were respectively 4.78 MPa and 10.73 GPa for the 3-D model, compared with 4.25 MPa and 10.57 GPa for the experiment. For the F.GC2 composite, the cracking stress (σ_I) and the initial stiffness (E_I) were respectively 5.31 MPa and 11.29 GPa for the 3-D model, compared with 6.38 MPa and 11.33 GPa for the experiment.

Regarding the ultimate tensile strength properties, the numerical model also had a close prediction for both carbon TRCs. For the case of the F.GC1 specimen, experimental and numerical results show respectively the values of 12.76 MPa and 13.09 MPa for the ultimate strength (σ_{UTS}) and 0.866% and 0.806% for the ultimate strain (σ_{UTS}). For the F.GC2 specimen, the ultimate strength (σ_{UTS}) and strain (σ_{UTS}) were 10.95 MPa and 0.889% for numerical results comparing with 10.30 MPa and 0.813% for the experimental data. Table 2 shows all the values of the mechanical properties obtained from the 3-D numerical model in comparison with the experimental data.

2.3.3 Failure modes

Thanks to the cracking model for the cementitious matrix, the 3-D numerical model could show the failure modes of TRC composites with multi-transversal cracks along the specimen's length. However, there was a difference in the network of cracks between the two carbon TRC composites, continuous crack system for F.GC2 and discontinuous one for F.GC1. This result was caused by the number and distance of textile warps on the TRC's cross-section: two textile warps with a distance of 46 mm for F.GC1 and three textile warps with a distance of 17 mm for F.GC2. The cracks occurred firstly at the cementitious matrix elements around the carbon textile warps, then widened towards the elements in the same cross-section, and finally finished when the cracks were complete. Thus, the network of cracks greatly depends on the number and distance of textile warps on the TRC's cross-section. With high textile density for F.GC2 specimen, almost TRC's cross-section completely cracked, leading to the continuous crack system. With low textile density for F.GC1 specimen, there were several uncracked elements of the cementitious matrix, leading to a discontinuous crack system. Fig. 6 presents the failure modes of carbon TRC specimens in both experimental and numerical results. From that, it could be found a remarkable agreement between both results.

2.3.4 Mechanical behaviour of carbon textile warps

From the numerical model, the global response of carbon textile could be identified as presented in Fig. 7 below. In the F.GC2 specimen, three GC2 textile warps behaved similarly at the first and second phases and a slight difference at the last one. Because of the redistribution of the tensile force after each crack, there were drops in the stress of three warps on the cracking phase of TRC's behaviour. However, it could be said that the axial stress of three textile warps was at the same level for all this phase. At the end of the cracking process, three GC2 warps had a jump in axial stress however at different levels. This jump caused by the complete cracking of the cementitious matrix. So, the tensile force in the matrix was transmitted to three textile warps, however at different levels depending on the position of these warps. That explains a slight difference between the stress-strain curves of three GC2 carbon textile warps.

2.4 Discussion

From the comparison of both numerical and experimental results in section 2.3, it could be said that the

Table 2 Comparison between both experimental and numerical results for the mechanical properties in three phases (Tran 2019)

TRC composite	First crack values			Post crack values					
	σ_I (MPa)	σ_I (%)	E_I (GPa)	σ_{II} (MPa)	σ_{II} (%)	E_{II} (GPa)	σ_{UTS} (MPa)	σ_{UTS} (%)	E_{III} (GPa)
F.GC1 – Numerical	4.78	0.047	10.73	5.72	0.400	0.27	13.09	0.806	1.78
F.GC1 - Experimental	4.25	0.071	10.57	6.16	0.536	0.55	12.76	0.866	3.04
F.GC2 – Numerical	5.31	0.079	11.29	5.89	0.370	0.27	10.95	0.889	1.43
F.GC2 - Experimental	6.38	0.083	11.33	7.51	0.671	0.33	10.30	0.813	2.50

(a) For F.GC1 composite

(b) For F.GC2 composite

Fig. 6 Failure modes of carbon TRC specimens in both experimental and numerical results

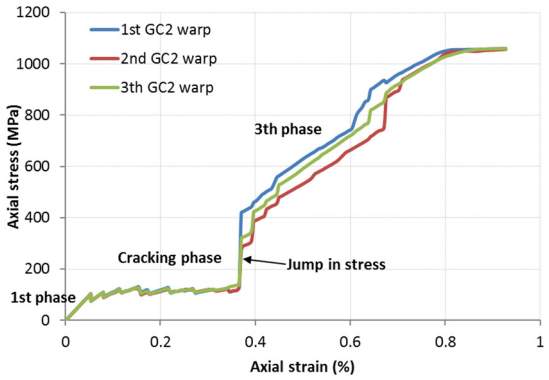

Fig. 7 Stress-strain relationship of three GC2 textile warps

3-D model provided a reliable result for predicting the tensile behaviour and mechanical properties of the TRC composite. This model also shows the failure mode with the cracking of the cementitious matrix, corresponding with the observation of TRC specimens after the tensile tests. Furthermore, it could be observed the occurring of cracks as well as the development of cracking zone. However, for the cracking phase, the deformation of the TRC specimen at the state of the end of the cracking was different from that in the experiment (see Fig. 3). This difference is due to the effect of the phenomena occurring in the cracking phase that the 3-D model could not consider. The dynamic phenomena after each crack appearance led to an increase in the tensile deformation of the specimen. Furthermore, the reinforcement textile would be pulled out from the cementitious matrix. This phenomenon also increased the overall deformation of the TRC specimen.

Another disadvantage of this 3-D model is the assumption of the perfect bonding between the textile reinforcement and the cementitious matrix. This assumption is based on the high bond strength on the surface between two materials related to the ultimate strength of the cementitious matrix, shown over the high density of multi-cracks. However, in some cases of studies as corrosion or at high temperatures, the together working between the textile and the matrix at the interface is not perfect as this assumption. This leads to a significant difference in global deformation between both numerical and experimental results. Furthermore, this model just corresponds with the TRC composite with the reinforcement of continuous fiber. In the case of reinforcement with discontinuous fiber, it needs to use a method of equivalent conversion from the reinforcement ratio for calculation steps.

3. Effect of studied parameters on TRC's behaviour

This section presents the parametric studies to consider the effects of parameters such as the position and length of the strain measurement zone, the thickness of the matrix layer and the elevated temperature, on the TRC's behaviour.

3.1 Effect of the position and length of the strain measurement zone

As analyzed in section 1.2, the strain measurement performance of each measurement instrument significantly influences the experimental result. Thus, the different

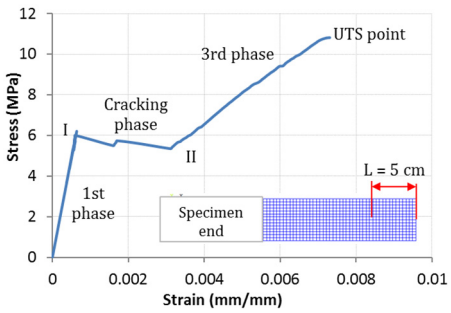

(a) Deformation measurement length of 5 cm in the middle

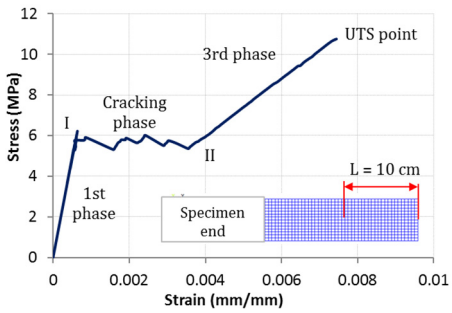

(b) Deformation measurement length of 10 cm in the middle

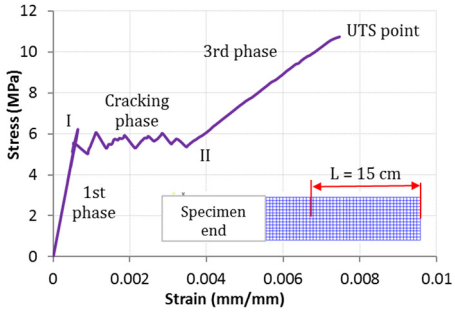

(c) Deformation measurement length of 15 cm in the middle

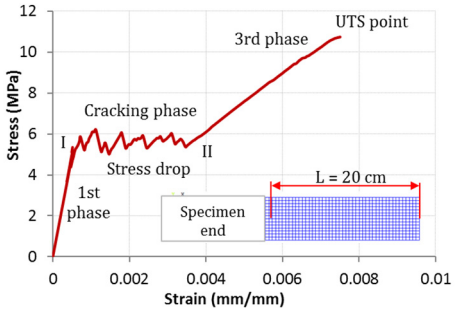

(d) Deformation measurement length of 20 cm in the middle

Fig. 8 Different shapes of stress-strain curves depending on the length of strain measurement zone

positions and lengths of the strain measurement zone could provide various results in the stress-strain curve and mechanical properties of the TRC composite. This parametric study was carried out by changing the position and length of the strain measurement zone in the 3-D numerical model. In this parametric study, the axial strain was determined from the displacement of the nodes on the surface of the TRC specimen with the strain measurement length from 5 cm to 20 cm.

Fig. 8 presents the different shapes of stress-strain curves depending on the length of strain measurement zone from 5 cm to 20 cm. From Fig. 8, a little difference in the cracking phase could be observed between all cases of strain measurement length. With the length of the strain measurement zone higher, the 3-D numerical model provided a higher deformation of the cracking phase and a greater number of cracks in the stress-strain curve. So, the distance between the two cracks was shortened in the cracking phase.

Concerning the effect of the position of the strain measurement zone, if the first cracks were not inside it, these cracks were recorded in the stress-strain curve with a wrong strain value. So, the cracking stress (s_I) could be identified from the stress-strain curve with a mistaken value. As a numerical result, the cracking stress value for the cases of 5 cm, 10 cm, and 15 cm was 6.21 MPa, while this value was the stress in the fourth crack. It means that with the strain measurement length of 5 cm, 10 cm, and 15 cm from the middle of TRC's specimen, the specimen deformation in the three first cracks were incorrect. So, it could be observed the cracking phase in the three first cracks, was a part of the linear phase (first phase) in Figs. 8(a)-(c). For the case of the strain measurement length of 20 cm in the middle, the cracking stress was 5.31 MPa, and all cracks were recorded in the stress-strain curve (see Fig. 8(d)).

This numerical result was in good agreement with the explanation of the experimental results in the works of Saidi and Gabor (2020). In this study, the data on TRCMC (Textile-Reinforced Cementitious Matrix Composite) with different strain measurement methods (DIC, strain gauge, optical fibre) were compared and analyzed (see Fig. 9). The experimental results released the different stress-strain curves obtained by DIC on the cracked and uncracked positions. This difference in the shape of the stress-strain curve was due to the difference in obtained deformation. The DIC deformation measured method used the displacement of points on the TRC specimen surface at the deformation measured zone to calculate the axial strain. At the uncracked position, the strain measured from DIC at the uncracked position did not increase, leading to the extraordinary curve. Contrarily, at the cracked position, the relative displacement between the two start and end points increased when the tensile force increased. So, the strain-hardening curve was in normal form. It means that the position of the strain measurement zone has influenced the shape of the stress-strain curve. On another hand, the experimental result obtaining from the strain gauge was similar to that of the cementitious matrix observing by optical fibre. This result showed that the strain measurement performance of the virtual gauge (throughout its measured length) was just enough to identify the first phase of the mechanical behaviour of the TRC composite. This is the effect of the position and length of the strain measurement zone on the TRC's behaviour.

3.2 Effect of the effective thickness of cementitious matrix for one textile layer

In order to consider the effect of the effective thickness

of the cementitious matrix on TRC's behaviour, a parametric study was carried out by changing the value of this thickness in six levels from 10 mm to 20 mm for F.GC2 composite. Corresponding with this range of thickness, the reinforcement ratio varies from 0.53% (20 mm of thickness) to 1.06% (10 mm of thickness). Fig 10 shows different shapes of stress-strain curves depending on the effective thickness of the matrix cementitious.

As the numerical results, the stress-strain curve transforms different shapes depending on the effective thickness of the cementitious matrix. When this value was higher than 16 mm, the numerical model provided a strain-softening behaviour with the cracking phase for the F.GC2 composite. It means that with a reinforcement ratio lower than 0.66%, the reinforcement of one textile layer was not enough for the cementitious matrix in these cases. With the effective thickness of 10 mm, 11.5 mm, 13.5 mm, and 15 mm corresponding with the reinforcement ratio higher than 0.70%, the F.GC2 composite presented a strain-hardening behaviour with three distinguished phases as in the literature. This result was in agreement with that presented in the study of Contamine (2011) concerning the critical values of reinforcement ratio.

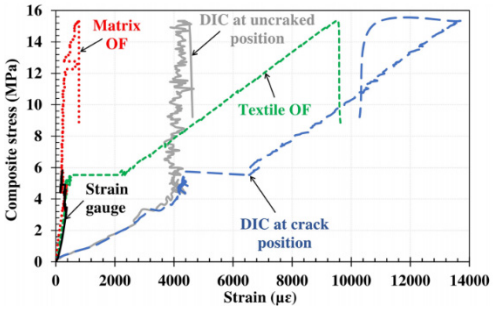

Fig. 9 Comparison between experimental results obtained from optical fibre, strain gauge, and DIC with virtual gauges (Saidi and Gabor 2020)

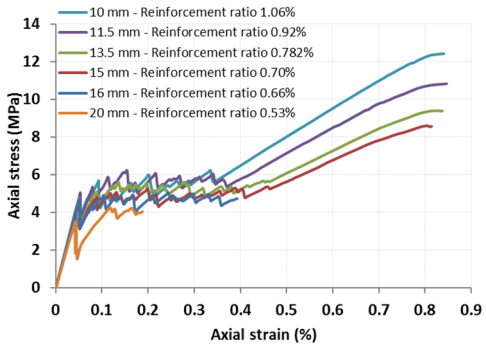

Fig. 10 Different shapes of stress-strain curves depending on the matrix cementitious thickness

From Fig. 10, it could be found the change of the tensile mechanical properties of the F.GC2 specimen depending on the thickness of the cementitious matrix. It is almost a reduction tendency for all TRC's characteristics. In the first phase, the cracking stress significantly decreased from 5.69 MPa down to 3.48 MPa while the Young's modulus slightly decreased from 11.52 GPa down to 8.44 GPa, corresponding with the increase of cementitious matrix thickness from 10 mm to 20 mm. For the ultimate tensile characteristics of F.GC2 composite, these values strongly reduced, from 12.54 MPa down to 4.25 MPa for axial strength and from 0.953% down to 0.188% for axial strain, corresponding with the thickness range from 10 mm to 20 mm. Concerning the shape of the cracking phase on the stress-strain curves, it was the same form for all cases of cementitious matrix thicknesses, however at different levels. When the matrix layer thickness increases, the cracking phase was slightly extended, but at a lower stress level. Table 3 presents all mechanical properties of F.GC2 composite corresponding with different cementitious matrix thicknesses from 10 mm to 20 mm.

3.3 Estimation of the elevated temperature behaviour of TRC composite

In the case of fire, the mechanical characteristics of constitutive materials gradually decrease with the increase of temperature, leading to the evolution of TRC's properties. From the numerical model, a parametric study was performed to estimate the elevated temperature behaviour of F.GC2 composite in the range of temperature from 25°C to 400°C. The experimental results in the authors' previous study showed that with a temperature lower than 400°C, the bonding strength between the GC2 textile and cementitious matrix was good enough to obtain the cracking phase on the strain-hardening curve (because

Table 3 Numerical results of parametric study on effect of the cementitious matrix thicknesses of the cementitious matrix

Results	First crack values			Post crack values					
	σ_I (MPa)	σ_I (%)	E_I (GPa)	σ_{II} (MPa)	σ_{II} (%)	E_{II} (GPa)	σ_{UTS} (MPa)	σ_{UTS} (%)	E_{III} (GPa)
F.GC2-10 mm Num	5.69	0.092	11.52	6.22	0.335	0.33	12.54	0.953	1.48
F.GC2-11.5 mm Num	5.31	0.079	11.29	5.89	0.370	0.27	10.95	0.889	1.43
F.GC2-11.5mm Exp	**6.38**	**0.083**	**11.33**	**7.51**	**0.671**	**0.33**	**10.30**	**0.813**	**2.50**
F.GC2-13.5 mm Num	4.75	0.051	9.28	5.35	0.384	0.29	9.39	0.809	1.06
F.GC2-15 mm Num	4.64	0.051	9.15	5.37	0.464	0.26	8.61	0.806	1.02
F.GC2-16 mm Num	4.72	0.052	9.02	4.74	0.394	0.23			
F.GC2-20 mm Num	3.48	0.041	8.44	4.25	0.188	0.21			

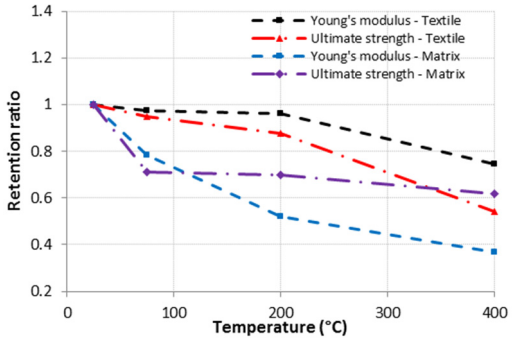

Fig. 11 Evolution of the mechanical properties of constitutive materials as a function of temperature (experimental data obtained by the authors' previous study (Tran *et al*. 2019))

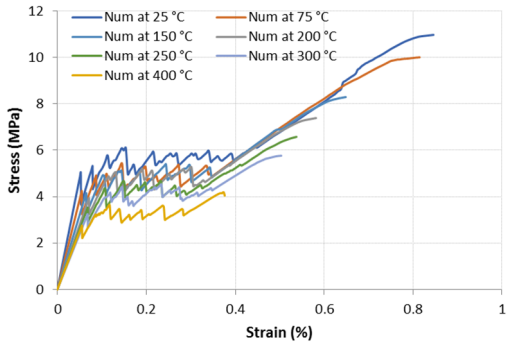

Fig. 12 Numerical results of stress-strain curves of the F.GC2 composite at different elevated temperatures from 3-D modelzz

the GC2 textile was treated with silica amorphous which improved the bonding strength between both materials). It means that the together working between the GC2 textile and the matrix at the interface could satisfy the assumption of the model. The input data for this study were firstly selected from Table 1 for the properties at room temperature. After that, the theirs evolution as a function of the elevated temperature was identified from the experimental results in the authors' previous study (Tran *et al*. 2019). Fig 11 below presents the evolution of these mechanical properties depending on the elevated temperature ranging from 25°C to 400°C.

Fig. 12 presents the stress-strain curves of F.GC2 composite estimated from a parametric study at elevated temperatures ranging from 25°C to 400°C. As the numerical result, the F.GC2 composite exhibited a strain-hardening behaviour for all cases of different temperatures. However, from Fig. 12, it could be found a gradual reduction in the mechanical properties of F.GC2 with the increase in elevated temperature levels. Concerning the ultimate strength of the F.GC2 composite, this value decreased from 10.95 MPa down to 4.03 MPa corresponding with the temperature increase from 25°C to 400°C. The ultimate strain was also in the reducing trend with the increase of elevated temperature, from 0.84% at 25°C to 0.38% at 400°C.

From Fig. 12, it could be found the gradual reduction of mechanical properties of the F.GC2 composite in the first phase (cracking stress, cracking strain, and initial stiffness). The cracking stress was 5.31 MPa at 25°C and 2.75 MPa at 400°C while Young's modulus decreased from 11.29 GPa down to 4.96 GPa in the temperatures ranging from 25°C to 400°C. The cracking phase was also shortened and at the lower stress levels when the temperature increases. In comparison with the experimental data at 75°C, 200°C and 400°C, the numerical result presents a good agreement. Fig. 13 below presents the comparison between the numerical results and the authors' previous experimental data for F.GC2 mechanical behaviour at 75°C, 200°C and 400°C.

4. Conclusions

This paper presents the numerical results concerning the tensile behaviour of the TRC composites by using a cracking model for the cementitious matrix. Firstly, the 3-D model was developed and validated with the authors' previous experimental data on two carbon TRC specimens. After that, this model was used to study the effects of several parameters belonging to the performance of the measurement equipment, specimen design, and environment. As numerical results, the following conclusions can be drawn for this work:

The effect of the length and position of the strain measurement zone was highlighted thanks to a parametric study by changing the value of this parameter. When this length extends, the cracking phase on the stress-strain curve recorded more cracks, and the length of this phase was extended. If the first cracks occurred outside the strain

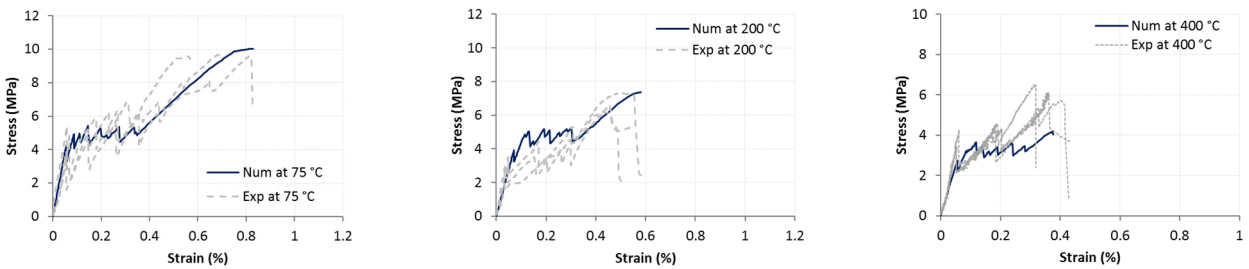

(a) For the case of 75°c (b) For the case of 200°C (c) For the case of 400°C

Fig. 13 Comparison between both experimental and numerical results for elevated behaviour of F.GC2

measurement zone, these cracks would not be recorded on the stress-strain curves. So, the cracking stress (s_I) would be identified by a wrong value from the stress-strain curve.

The effective thickness of the matrix layer per one carbon textile varies from 10 mm to 20 mm, leading to the reduction of the reinforcement ratio, effected to the shape of the stress-strain curve. It transformed from the strain-hardening behaviour to the strain-softening one. The mechanical properties of carbon TRC composite also decreased gradually with the raising of this thickness. The cracking phase was slightly extended but at a lower level.

The elevated temperature behaviour of the TRC composite could be estimated from the 3-D numerical model. As result, the TRC composite exhibited a strain-hardening behaviour for all cases of different temperatures. The cracking phase was also shortened and at a lower level. All mechanical properties of TRC composite gradually decreased by about 50% their value with the increase of temperature from 25°C to 400°C.

For future works, it will be interesting to build a numerical model to estimate the mechanical behaviour of reinforced concrete (RC) members strengthening with TRC composites under shear or/and flexural loadings. With this model, it would be identified the efficacy of the TRC composite for strengthening RC members.

Acknowledgments

This research has been performed with the support of LMC2 laboratory for the experimental and numerical works and with financial support of the Ministry of Education and Training of Vietnam to the first author, Grant No. B2021-MDA-10.

References

ANSYS (2011), Mechanical APDL element reference, Vol. 14.

Brameshuber, W. (2006), "Textile reinforced concrete - State-of-the-Art", Report of RILEM TC 201-TRC.

Caggegi, C. Lanoye, E., Djama, K., Bassil A. and Gabor, A. (2017), "Tensile behaviour of a basalt TRM strengthening system: Influence of mortar and reinforcing textile ratios", *Compos. Part B: Eng.*, **130**, 90-102. https://doi.org/10.1016/j.compositesb.2017.07.027

Colombo, I.G., Magri, A., Zani, G., Colombo, M. and di Prisco, M. (2013), "Erratum to: Textile reinforced concrete: Experimental investigation on design parameters", *Mater. Struct.*, **46**(11), 1953-1971. https://doi.org/10.1617/s11527-013-0023-7

Colombo, I.G., Colombo, M., di Prisco, M. and Pouyaei, F. (2018), "Analytical and numerical prediction of the bending behaviour of textile reinforced concrete sandwich beams", *J. Build. Eng.*, **17**, 183-195. https://doi.org/10.1016/j.jobe.2018.02.012

Contamine, R. (2011), "Contribution à l'étude du comportement mécanique de composites textile-mortier : application à la réparation et/ou renforcement de poutres en béton armé vis-à-vis de l'effort tranchant", Ph.D. Thesis; Université Claude Bernard - Lyon I.

Contamine, R., Larbi, A.S. and Hamelin, P. (2011), "Contribution to direct tensile testing of textile reinforced concrete (TRC) composites", *Mater. Sci. Eng.: A*, **528**(29-30), 8589-8598. https://doi.org/10.1016/j.msea.2011.08.009

Djamai, Z.I., Bahrar, M., Salvatore, F., Si Larbi, A. and El Mankibi, M. (2017), "Textile reinforced concrete multiscale mechanical modelling: Application to TRC sandwich panels", *Finite Elem. Anal. Des.*, **135**, 22-35. https://doi.org/10.1016/j.finel.2017.07.003

Douk, N., Vu, X.H., Si Larbi, A., Audebert, M. and Chatelin, R. (2021), "Numerical study of thermomechanical behaviour of reinforced concrete beams with and without textile reinforced concrete (TRC) strengthening: Effects of TRC thickness and thermal loading rate", *Eng. Struct.*, **231**, 1117-1137. https://doi.org/10.1016/j.engstruct.2020.111737

Ehlig, D., Jesse, F. and Curbach, M. (2010), "High temperature tests on textile reinforced concrete (TRC) strain specimens", In: Aachen University, pp. 141-151.

Ferrara, G., Caggegi, C., Gabor, A. and Martinelli, E. (2019), "Experimental study on the adhesion of basalt textile reinforced mortars (TRM) to clay brick masonry: The influence of textile density", *Fibers*, **7**(12), 103. https://doi.org/10.3390/fib7120103

Giese, A.C.H., Giese, D.N., Dutra, V. and Filho, D. (2021), "Flexural behavior of reinforced concrete beams strengthened with textile reinforced mortar", *J. Build. Eng.*, *33*, 1018-1073. https://doi.org/10.1016/j.jobe.2020.101873

Halim, N.H.F.A., Alih, S.C. and Vafaei, M. (2021), "Seismic behavior of RC columns internally confined by CFRP strips" *Adv. Concrete Constr., Int. J.*, **12**(3), 217-225. https://doi.org/10.12989/acc.2021.12.3.217

Jawahery, M.S.A., Çevik, A. and Gülşan, M.E. (2022), "3D FE modeling and parametric analysis of steel fiber reinforced concrete haunched beams", *Adv. Concrete Constr., Int. J.*, **13**(1), 45-69. https://doi.org/10.12989/acc.2022.13.1.045

Li, B., Xiong, H., Jiang, J. and Doua. X. (2019), "Tensile behavior of basalt textile grid reinforced engineering cementitious composite", *Compos. Part B: Eng.*, **156**, 185-200. https://doi.org/10.1016/j.compositesb.2018.08.059

Li, Y., Yin, S., Dai, J. and Liu, M. (2020), "Numerical investigation on the influences of different factors on the seismic performance of TRC-strengthened RC columns", *J. Build. Eng.*, **30**, 1012-1045. https://doi.org/10.1016/j.jobe.2020.101245

Mechtcherine, V. (2013), "Novel cement-based composites for the strengthening and repair of concrete structures", *Constr. Build. Mater.*, **41**, 365-373. https://doi.org/10.1016/j.conbuildmat.2012.11.117

Portal, N.W., Flansbjer, M., Johannesson, P., Malaga, K. and Lundgren, K. (2016), "Tensile behaviour of textile reinforcement under accelerated ageing conditions", *J. Build. Eng.*, **5**, 57-66. https://doi.org/10.1016/j.jobe.2015.11.006

Portal, N.W., Thrane, L.N. and Lundgren, K. (2017), "Flexural behaviour of textile reinforced concrete composites: Experimental and numerical evaluation", *Mater. Struct.*, **50**(1), 1-14. https://doi.org/10.1617/s11527-016-0882-9

Rambo, D.A.S., de Andrade Silva, F., Toledo Filho, R.D. and Gomes, O. (2014), "Effects of elevated temperatures on the interface properties of carbon textile-reinforced concrete", *Cement Concrete Compos.*, **48**, 26-34. https://doi.org/10.1016/j.cemconcomp.2014.01.007

Rambo, D.A.S., Yao, Y., de Andrade Silva, F., Toledo Filho, R.D. and Mobasher, B. (2017), "Experimental investigation and modelling of the temperature effects on the tensile behavior of textile reinforced refractory concretes", *Cement Concrete Compos.*, **75**, 51-61. https://doi.org/10.1016/j.cemconcomp.2016.11.003

Saidi, M. and Gabor, A. (2019), "Use of distributed optical fibre as a strain sensor in textile reinforced cementitious matrix composites", *Measurement*, **140**, 323-333.

https://doi.org/10.1016/j.measurement.2019.03.047

Saidi, M. and Gabor, A. (2020), "Adaptation of the strain measurement in textile reinforced cementitious matrix composites by distributed optical fibre and 2D digital image correlation", *Strain*, **56**(1), e12335. https://doi.org/10.1111/str.12335

Tlaiji, T., Vu, X.H., Ferrier, E. and Si Larbi, A. (2018), "Thermomechanical behaviour and residual properties of textile reinforced concrete (TRC) subjected to elevated and high temperature loading: Experimental and comparative study", *Compos. Part B: Eng.*, **144**, 99-110. https://doi.org/10.1016/j.compositesb.2018.02.022

Tran, M.T. (2019), "Caractérisation expérimentale et modélisation numérique du comportement thermomécanique à haute température des matériaux composites renforcés par des fibres", Ph.D. Thesis; Université de Lyon.

Tran, M.T., Vu, X.H. and Ferrier, E. (2019), "Mesoscale experimental investigation of thermomechanical behaviour of the carbon textile reinforced refractory concrete under simultaneous mechanical loading and elevated temperature", *Constr. Build. Mater.*, **217**, 156-171. https://doi.org/10.1016/j.conbuildmat.2019.05.067

Tran, M.T., Do, N.T., Dinh, T.T.H., Vu, X.H. and Ferrier, E. (2020a), "A 2-D numerical model of the mechanical behavior of the textile-reinforced concrete composite material: effect of textile reinforcement ratio", *J. Min. Earth Sci.*, **61**(3), 47-56. https://doi.org/10.46326/JMES.2020.61(3).06

Tran, M.T., Vu, X.H. and Ferrier, E. (2020b), "Mesoscale numerical modeling and characterization of the effect of reinforcement textile on the elevated temperature and tensile behaviour of carbon textile-reinforced concrete composite", *Fire Safe. J.*, **116**, 103186. https://doi.org/10.1016/j.firesaf.2020.103186

Tran, M.T., Vu, X.H., Dao, P.L. and Pham, D.T. (2021), "A 3-D finite element modeling for the textile-reinforced concrete plates under tensile load using a non-linear behaviour for cementitious matrix", *J. Sci. Technol. Civil Eng.* (*STCE*) - *NUCE*, **15**(1), 67-78. https://doi.org/10.31814/stce.nuce2021-15(1)-06

Truong, B.T. (2016), "Formulation, performances mécaniques, et applications, d'un matériau TRC pour le renforcement et la réparation de structures en béton/et béton armé : Approches expérimentale et numérique", Ph.D. Thesis; Université de Lyon.

William, K.J. and Warnke, E.P. (1975), "Constitutive model for the triaxial behavior of concrete", In: Association of Bridge and Structural Engineers, Seminar on Concrete Structure subjected to Triaxial Stresses, Paper III-1, Bergamo, Italy.

JHK